PENETRATION PHENOMENA IN TEFLON AND ALUMINUM FILMS USING 50-3200 μm GLASS PROJECTILES;
Friedrich Hörz[1], Scott Messenger[2], Ron Bernhard[3], Thomas H. See[3], and Gerald Haynes[3]; [1]NASA/JSC, Houston, TX 77058; [2]Univ. Washington, Seattle 98195; [3]Lockheed ESC, C23, 2400 NASA Road 1, Houston, TX 77058.

INTRODUCTION: Protective thermal blankets and other thin membranes retrieved from space exhibit numerous penetration holes caused by natural and man-made hypervelocity particles (1,2). Interpretation of the hole diameters, regarding projectile dimensions and associated mass, relies on laboratory simulations to determine empirically how penetration-hole size relates to projectile dimensions and other initial conditions (*e.g.,* see summary by [3]). We have added to the existing data in two ways by: (1) employing projectiles from 50 to 3200 μm in diameter to complement existing data from electrostatic accelerators (typically <1 μm projectiles, *e.g.,* [3,4]) and light-gas guns (typically >>1000 μm projectiles; e.g., [5]); and (2) exclusively using soda-lime glass projectiles, while most previous data was derived *via* metal impactors. Our choice of target membranes relates to ongoing flight opportunities. Teflon was chosen because the Long Duration Exposure Facility (LDEF) returned ~16 m^2 of Teflon thermal blankets, while aluminum was used because thin Al foils are contemplated for the proposed Cosmic Dust Collection Facility (CDCF) on the Space Station (6).

EXPERIMENTS: A 5 mm bore light-gas gun was used to launch all projectiles with those ≥500 μm in diameter being launched individually, while an ensemble of typically 30-80 particles was accelerated for smaller sized projectiles, of which only a few (typically 2-5) encountered the target film. A photo-diode detected the lightflash of individual spheres as small as 50 μm, as does an electrostatic grid that monitored the plasma/electrons generated upon foil impact. The velocity range between the fastest and slowest projectile for any given experiment is <2% and typically <1%. All experiments were conducted at velocities between 5.8 and 6.2 km/s, at normal incidence relative to the test film, and employed a witness plate mounted at a known distance behind the foil. This report describes the impact feature(s) on the test foil; analysis of the witness-plates is described in a companion abstract (7). The following definitions apply: T_f = Foil Thickness, D_p = Projectile Diameter, D_c = Crater Diameter (at original target surface), D_r = Rim Crest-To-Rim Crest distance, D_s and D_l reflect the average diameters of the Spall zone (in Teflon) or the plastically deformed crater-Lip (in aluminum), and D_h = Penetration-Hole diameter.

RESULTS: Figure 1 illustrates the systematic decrease in penetration-hole diameter for identical 150 μm projectiles encountering increasingly thinner 1100-series Al foils as indicated by D_p/T_f in the lower right-hand corner. Also note the systematic decrease in relative rim-width compared to the hole dimensions. Essentially identical phenomena occur with Teflon targets; however, Teflon behaves brittlely and develops substantial spall zones in place of plastically deformed crater lips. Diameter measurements, all scaled to projectile dimensions, are illustrated in Figure 2 for Al, and in Figure 3 for Teflon targets. Note that D_c grades gradually into D_h in the case of Al, and that D_r and D_l approach D_h with decreasing foil thickness. Hole dimensions approximate those of the projectile when D_p/T_f >30. Similar trends are observed for the Teflon targets. Note that two Teflon experiments (at D_p/T_f = 0.2-0.5) resulted in penetration holes that are significantly smaller than the corresponding crater diameters. In addition, substantial spallation is observed with >1000 μm projectiles into Teflon resulting in penetration holes with jagged outlines, and making the precise measurement of a diameter somewhat difficult.

IMPLICATIONS: The trends displayed in Figures 2 and 3 argue for a gradual and highly systematic transition from a true cratering regime in thick targets to one of simply dislodging the cross-sectional area of the projectile in very thin foils. This systematic behavior will permit unique solutions for (unknown) D_p from surfaces retrieved from space as illustrated *via* Figure 4, which plots the measurable parameters (D_h and T_f) essentially against D_p. Note the substantial convergence of all data at relatively thin foils. This merely illustrates that physical properties of specific foil materials become increasingly less important, if not insignificant, with ever decreasing foil thickness. On the other hand, specific material properties strongly control crater growth and will affect the morphology of craters in infinite halfspace targets, as well as the morphology of penetration holes in relatively massive membranes. Some of the scatter in Figure 4 (at thick foils) relates to (not yet corrected) differences in impact velocities (5.8 versus 6.2 km/s), yet most scatter in the Teflon shots is caused by difficulties in precisely defining D_h. By and large, the relationships between D_p, T_f and D_h scale nicely with absolute dimensions over a range in D_p from 50 to 3175 μm and foil thicknesses from 1 to 10,000 μm. Also illustrated in Figure 4 is the penetration formula of Carey *et al.,* ([3]; equation 10 suitably adjusted to our experimental conditions for aluminum foils) largely derived from <1 μm and >>1mm diameter metal projectiles. The agreement is excellent.

Most penetrations on space-exposed surfaces to date are characterized by D_h/T_f <5 and are thus substantially affected by material-dependent cratering phenomena. Reliable and unique determination of D_p seems to require dedicated impact experiments for each (major) material type recovered from low-Earth orbit, as important secondary criteria, largely resulting from the cratering process, may be established, such as spall dimensions, lip-width, etc., to further characterize the nature of the penetration and the size of the impactor.

REFERENCES: (1) Warren J.L. *et al.* (1989), *Proceed. 19th LPSC*, p. 641-657; (2) See, T.H. *et al.* (1990), *LDEF M&D SIG Report*, JSC Publication No. 24608, 583 p.; (3) Carey, W.C. *et al.* (1985), in *Properties and Interactions of Interplanetary Dust,* p.131-136, Reidel Publ. Co.; (4) Pailer, N.M. and Grun, E. (1980), *Planet.Space Sci. 28*, 321-331; (5) Cour-Palais, B.G.(1987) *Int. Jorn. Impact Eng. 5*, 681-692; (6) *CDCF Steering Committee* (1990), NASA TM 102160, 29 p., (7) Messenger, S.R. and Hörz, F., this volume.

Figure 1

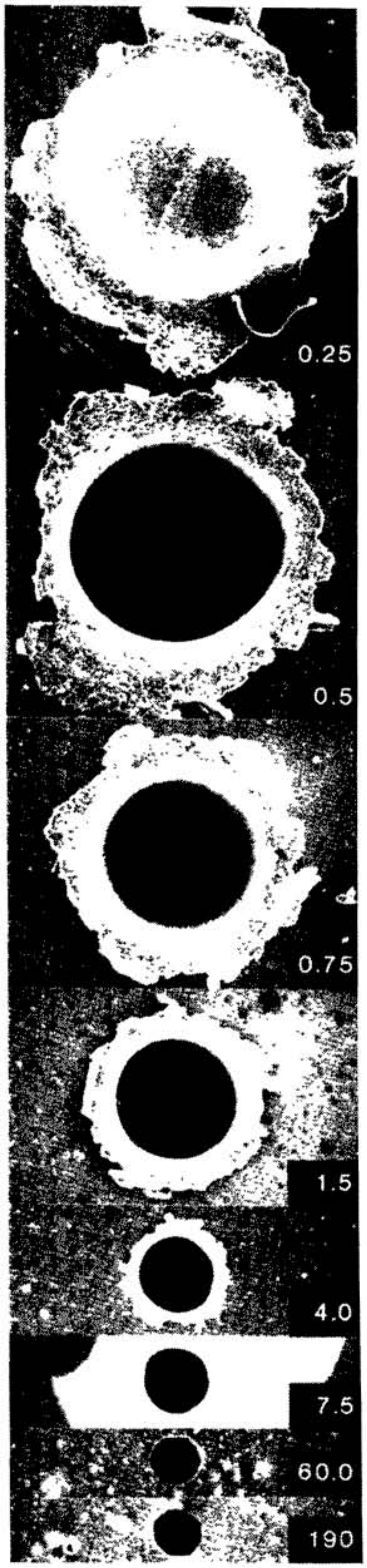
0.25
0.5
0.75
1.5
4.0
7.5
60.0
190

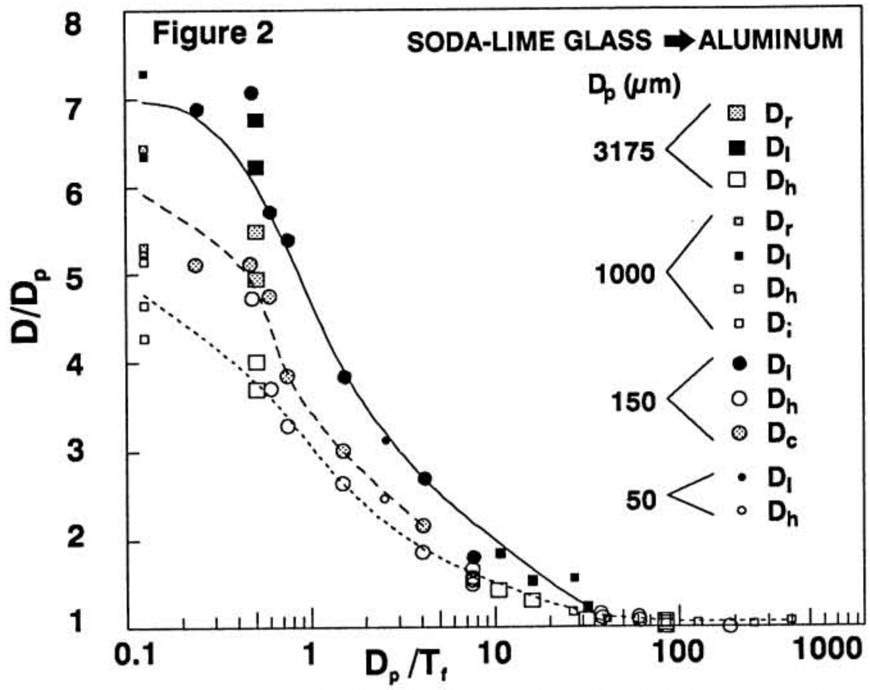
Figure 2
SODA-LIME GLASS ➡ ALUMINUM
D/Dp
Dp /Tf
Dp (μm)
3175
Dr
Dl
Dh
1000
Dr
Dl
Dh
Di
150
Dl
Dh
Dc
50
Dl
Dh
0.1
1
10
100
1000

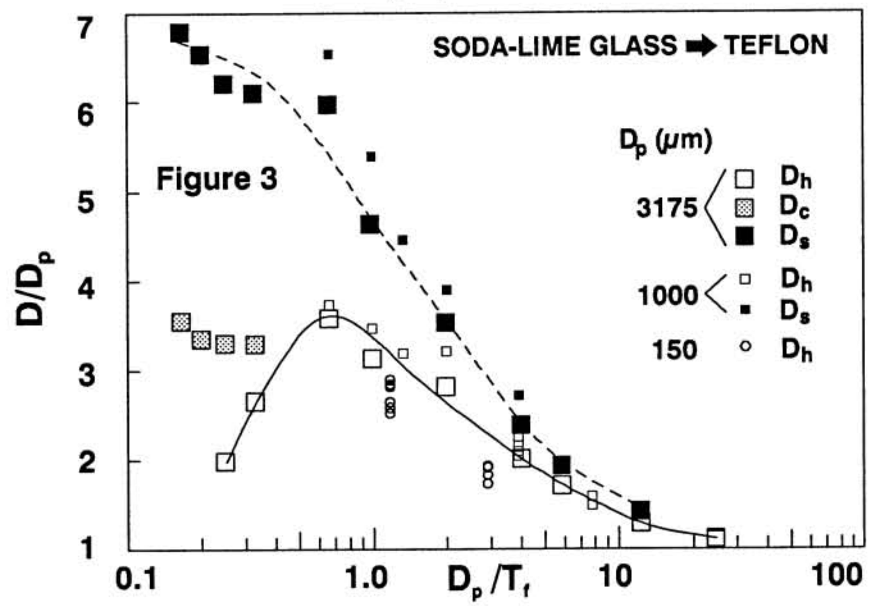
Figure 3
SODA-LIME GLASS ➡ TEFLON
D/Dp
Dp /Tf
Dp (μm)
3175
Dh
Dc
Ds
1000
Dh
Ds
150
Dh
0.1
1.0
10
100

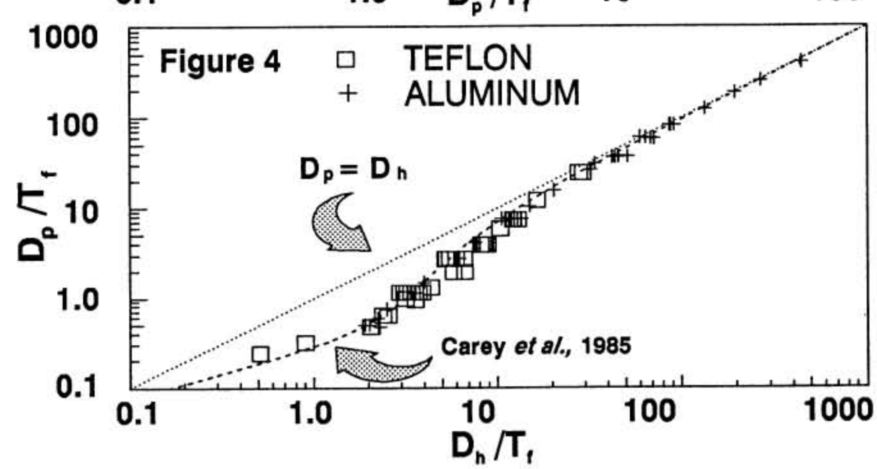
Figure 4
TEFLON
ALUMINUM
Dp = Dh
Carey et al., 1985
Dp /Tf
Dh /Tf
0.1
1.0
10
100
1000